

# Impact of the Frequency-Dependent Soil Electrical Properties on the Electromagnetic Field Propagation in Underground Cables

T. A. Papadopoulos, Z. G. Datsios, A. I. Chrysochos, P. N. Mikropoulos, G. K. Papagiannis

**Abstract--** In electromagnetic transient analysis, a major issue is the influence of the imperfect earth on the propagation characteristics of conductors. Although soil electrical properties present significant frequency-dependent (FD) behavior, in most cases earth is considered with constant properties. In this paper, the impact of the FD soil properties on the propagation characteristics of underground cables is investigated. For this purpose, generalized earth formulations are considered, taking into account the impact of earth conduction effects on both series impedance and shunt admittance of cable conductors. Comparisons are carried out using different FD soil models, also constant soil properties and with approximate earth formulations, neglecting the influence of imperfect earth on shunt admittances. Finally, transient simulations are performed to evaluate the impact of the different approaches.

**Keywords:** Earth conduction effects, electromagnetic transients, frequency-dependent soil models, cables.

## I. INTRODUCTION

STUDIES of electromagnetic (EM) transients in power systems require the accurate calculation in a wide frequency range of the parameters of system components. Among them, the series impedance and shunt admittance of transmission lines are probably the most crucial. Considering underground cable systems, Pollaczek first proposed formulas for the calculation of the series self and mutual impedance, assuming earth as a perfect conductor [1]. Later, Sunde [2] included in Pollaczek's formulas the influence of earth permittivity. Pollaczek's and Sunde's formulations are implemented in the routines of ATP-EMTP and EMTP-RV, respectively. However, the accuracy of these pioneering approaches is limited to the low-frequency (LF) range, since the influence of the imperfect earth on the shunt admittance is

neglected.

Earth models involving earth correction terms for the shunt admittance of underground power cables have been proposed in [3]-[7]; systematic investigations using these models have been presented in [8], [9]. In these studies, the electrical properties of soil, that is, resistivity and permittivity, were considered constant, although, it is well established that they are frequency-dependent (FD).

Several models have been proposed for the prediction of the FD soil electrical properties [10]-[13], as summarized in [14]. These models were applied to investigate the transient performance of overhead transmission lines [15]-[17] and grounding systems [14] subjected to lightning surges. It is important that the effects of the dispersion of soil electrical properties on EM propagation in underground cables [18] have been investigated only poorly so far.

This paper investigates the propagation characteristics of underground cables as affected by the FD soil electrical properties, by adopting the generalized formulation of earth return impedance and shunt admittance proposed in [5]. The widely applied FD soil model developed by Longmire and Smith [11], as well as those proposed in [12] and [13] have been employed for calculating the propagation characteristics of underground cables. Neglecting the influence of imperfect earth on the cable shunt admittance was also examined. Results are discussed through comparisons based on the adopted soil models and EM simulations of the transient response of an underground cable variable in length.

## II. EARTH IMPEDANCE AND ADMITTANCE PARAMETERS

A single core (SC) cable buried in a homogeneous earth, as shown in Fig. 1, is considered as a case study. The per-unit-length self-earth impedance and admittance of the cable are derived by (1) and (2), respectively, by replacing  $h_i$  and  $h_j$  with the burial depth  $h$  [5]:

$$Z'_e = \frac{j\omega\mu_m}{2\pi} \int_0^{+\infty} F_e(\lambda) \cos(y_{ij}\lambda) \cdot d\lambda, \quad (1)$$

$$Y'_e = j\omega P_e^{-1}, \quad (2)$$

$$F_e(\lambda) = \frac{e^{-\alpha'_1|h_i-h_j|} - e^{-\alpha'_1(h_i+h_j)}}{\alpha'_1} + \frac{2\mu_0 e^{-\alpha'_1(h_i+h_j)}}{\alpha'_1\mu_0 + \alpha'_0\mu_1}, \quad (3)$$

$$P_e = \frac{j\omega}{2\pi(\sigma_1 + j\omega\epsilon_1)} \int_0^{+\infty} [F_e(\lambda) + G_e(\lambda)] \cos(y_{ij}\lambda) \cdot d\lambda, \quad (4)$$

T. A. Papadopoulos is with the Power Systems Laboratory, Department of Electrical and Computer Engineering, Democritus University of Thrace, Xanthi 67100, Greece (e-mail: thpapad@ee.duth.gr).

Z. G. Datsios, P. N. Mikropoulos, and G. K. Papagiannis are with the School of Electrical and Computer Engineering, Aristotle University of Thessaloniki, Thessaloniki 54124, Greece (e-mail: zdatsios@auth.gr, pnm@eng.auth.gr, grigoris@eng.auth.gr).

A. I. Chrysochos is with Cablel® Hellenic Cables S.A., Viohalco Group, Maroussi 15125, Athens, Greece, (e-mail: achrysochos@fulgor.vionet.gr).

The work of A. I. Chrysochos was conducted in the framework of the act "Support of Post-Doc Researchers" under the Operational Program "Human Resources Development, Education and Lifelong Learning 2014-2020", which is implemented by the State Scholarships Foundation and co-financed by the European Social Fund and the Hellenic Republic.

$$G_e(\lambda) = \frac{2\mu_0\mu_1\alpha_1'(\gamma_1^2 - \gamma_0^2)e^{-\alpha_1'(h_i+h_j)}}{(a_1'\mu_0 + a_0'\mu_1)(a_1'\gamma_0^2\mu_1 + a_0'\gamma_1^2\mu_0)} \quad (5)$$

where  $a_k' = \sqrt{\lambda^2 + \gamma_k^2 + k_x'^2}$  and  $k_x' = \omega\sqrt{\mu_1\epsilon_1}$ . The EM properties of air are denoted as  $\epsilon_0$ ,  $\mu_0$  ( $\sigma_0 = 0$ ) and those of the homogeneous earth as  $\epsilon_1$ ,  $\mu_1$  and  $\sigma_1$ ; the corresponding propagation constants are defined as:

$$\gamma_m = \sqrt{j\omega\mu_m(\sigma_m + j\omega\epsilon_m)} \quad (6)$$

with  $m$ : 0 and 1 for air and earth, respectively.

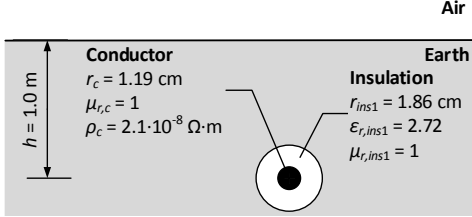


Fig. 1. Layout and characteristics of the single core cable.

### III. FREQUENCY-DEPENDENT SOIL MODELS

Soil is a dispersive lossy dielectric material with unity relative magnetic permeability. Thus, for EM transient studies, soil is characterized by its FD electrical properties: relative permittivity,  $\epsilon_{r1}$ , and effective conductivity,  $\sigma_1$  or resistivity,  $\rho_1$ . Several models have been reported in literature for the prediction of the FD electrical properties of soil. In this work the Longmire and Smith [11] (LS), Portela's [12] (POR), and the Alipio and Visacro [13] (AV) models have been adopted.

The LS model [11] was developed based on laboratory measurements performed by Scott [10] and Wilkenfeld [11] (frequency range: 100–2·10<sup>8</sup> Hz). According to this model,  $\epsilon_{r1}$  and  $\sigma_1$  (S/m) are given by (7) and (8), verified using circuit analysis:

$$\epsilon_{r1}(f) = \epsilon_{r1,\infty} + \sum_{n=1}^{13} \frac{a_n}{1 + (f/f_n)^2}, \quad (7)$$

$$\sigma_1(f) = \sigma_{1,DC} + 2\pi f \epsilon_0 \sum_{n=1}^{13} \frac{a_n f / f_n}{1 + (f/f_n)^2}. \quad (8)$$

In (7) and (8)  $\epsilon_{r1,\infty}$  is the relative permittivity of soil at high frequencies (HF), note that a HF value equal to 5 is proposed in [11],  $\sigma_{1,DC}$  (S/m) is the DC soil conductivity,  $a_n$  (p.u.) are empirical coefficients with values listed in Table I and  $f_n$  (Hz) are scaling coefficients given in [14] as:

$$f_n = 10^{n-1} (125\sigma_{1,DC})^{0.8312}. \quad (9)$$

The POR model [12] was derived on the basis of measurements conducted on undisturbed soil samples from several regions in Brazil (frequency range: 100–2·10<sup>6</sup> Hz). The soil properties  $\epsilon_{r1}$  and  $\sigma_1$  (S/m) are given as:

$$\epsilon_{r1}(f) = \frac{\beta_p \tan(\pi a_p / 2) \cdot 10^{-6} \cdot (2\pi f)^{a_p - 1}}{\epsilon_0}, \quad (10)$$

$$\sigma_1(f) = [\sigma_{1,LF} + \beta_p (2\pi f)^{a_p}] \cdot 10^{-6} \quad (11)$$

where  $\sigma_{1,LF}$  ( $\mu$ S/m) is the soil conductivity at LF (specifically at 100 Hz),  $a_p$  (p.u.) and  $\beta_p$  ( $s^{a_p} \cdot \mu$ S/m) are empirical coefficients with values depending on the tested soil. In this study,  $a_p$  and  $\beta_p$  are taken as 0.72 p.u. and 0.1 s<sup>0.72</sup>· $\mu$ S/m, respectively.

Alipio and Visacro [13] performed field measurements of the electrical properties of soil at several locations in Brazil (frequency range: 100–4·10<sup>6</sup> Hz). Based on mean measurement results, the following empirical expressions were proposed for  $\epsilon_{r1}$  and  $\sigma_1$  (S/m):

$$\epsilon_{r1}(f) = \epsilon_{r1,\infty} + \frac{1.26 \cdot 10^{-3} \tan(\pi \gamma_{AV} / 2) \sigma_{1,LF}^{0.27} f^{\gamma_{AV} - 1}}{2\pi \epsilon_0 \cdot 10^{6\gamma_{AV}}}, \quad (12)$$

$$\sigma_1(f) = [\sigma_{1,LF} + 1.26 \sigma_{1,LF}^{0.27} (f/10^6)^{\gamma_{AV}}] \cdot 10^{-3} \quad (13)$$

where  $\epsilon_{r1,\infty}$  is the relative permittivity of soil at HF (a HF value equal to 12 is proposed in [13]),  $\sigma_{1,LF}$  (mS/m) is the soil conductivity at LF (specifically at 100 Hz) and  $\gamma_{AV}$  (p.u.) is an empirical coefficient equal to 0.54 p.u. Note that in (7)-(13)  $f$  is the frequency in Hz.

#### A. Examined soil cases

Several soils differing in electrical properties were assumed; the properties of the soil cases are given in Table II. In Cases #1.1 and #1.2,  $\rho_1$  and  $\epsilon_{r1}$  are considered constant, with  $\rho_1=100$   $\Omega$ m and  $\epsilon_{r1}$  taking values 15 and 43, respectively. The value of 15 for  $\epsilon_{r1}$  is considered as typical in [19] for  $\rho_1 = 100$   $\Omega$ m, whereas that of 43 is obtained for  $\epsilon_{r1}$  at 1 MHz from the LS model. In Case #1.3,  $\rho_1$  and  $\epsilon_{r1}$  are considered as frequency-dependent, with  $\rho_1=100$   $\Omega$ m at 100 Hz. Specifically, for this case, soil electrical properties are estimated in the frequency range of 1 kHz to 1 MHz, by applying the three FD soil models, as described by (7)-(13). In an analogous way, by using  $\rho_1=1000$   $\Omega$ m, Cases #2.1-#2.3 have also been assumed.

#### B. Comparison of soil properties

Figs. 2a and 2b show  $\rho_1$  and  $\epsilon_{r1}$ , respectively, as a function of frequency for the Cases #1.3 and #2.3. Note that  $\rho_{1,DC}$  in the LS model is selected equal to 104.8  $\Omega$ m for Case #1.3 and 1097  $\Omega$ m for Case #2.3, so as to yield  $\rho_1$  values equal to 100  $\Omega$ m and 1000  $\Omega$ m at 100 Hz, respectively.

Regarding soil resistivity results of Fig. 2a,  $\rho_1$  decreases with frequency, especially when the  $\rho_{1,LF}$  is 1000  $\Omega$ m; thus, as  $\rho_{1,LF}$  increases the dependence of  $\rho_1$  on frequency becomes more intense. Deviations in the estimates of  $\rho_1$  among FD soil models increase with  $\rho_{1,LF}$  and frequency; the most pronounced dependence of  $\rho_1$  on frequency is predicted by the POR model.

From Fig. 2b it is evident that  $\epsilon_{r1}$  decreases drastically with frequency, with the rate of decrease varying among models. The high  $\epsilon_{r1}$  values can be attributed to interfacial polarization;

TABLE I  
EMPIRICAL COEFFICIENT VALUES FOR THE LS [11] SOIL MODEL

$n$	1	2	3	4	5	6	7	8	9	10	11	12	13
$a_n$	3.40	2.74	2.58	3.38	5.26	1.33	2.72	1.25	4.80	2.17	9.80	3.92	1.73
(p.u.)	$\times 10^6$	$\times 10^5$	$\times 10^4$	$\times 10^3$	$\times 10^2$	$\times 10^2$	$\times 10^1$	$\times 10^1$	$\times 10^0$	$\times 10^0$	$\times 10^{-1}$	$\times 10^{-1}$	$\times 10^{-1}$

TABLE II  
PROPERTIES OF EXAMINED SOIL CASES

Case	$\rho_1$ ( $\Omega$ m)	$\epsilon_{r1}$
#1.1	100	15
#1.2	100	43
#1.3	FD: 100 @ 100 Hz	FD
#2.1	1000	5
#2.2	1000	23
#2.3	FD: 1000 @ 100 Hz	FD

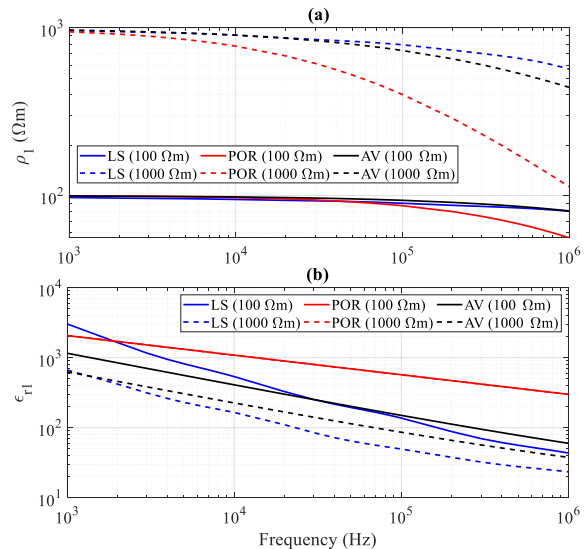


Fig. 2. Soil electrical properties: (a)  $\rho_1$  and (b)  $\epsilon_{r1}$  calculated by the three FD soil models.

such values are commonly measured at LF [20]. As also can be deduced from (10), the POR model yields estimates of  $\epsilon_{r1}$  which are independent of LF soil resistivity; this is not the case for the LS and AV soil models, where  $\epsilon_{r1}$  is lower for higher soil resistivity. The highest dispersion of soil electrical properties is observed for the LS model. The predicted behavior of soil electrical properties by the LS and AV models is in line with that experimentally obtained in [20], [21].

### C. Comparison of propagation characteristics

In Fig. 3 the cable attenuation constant, velocity and characteristic impedance magnitude are presented for soil Case #2.3, using the three examined FD soil models. The LS and AV models yield generally similar results up to 300 kHz. For higher frequencies there are differences between the two models, especially in the cable velocity (Fig. 3b) and characteristic impedance (Fig. 3c). The POR soil model results deviate from those obtained from LS and AV models, starting from the frequency of 10 kHz and becoming more pronounced in the HF range. This is attributed mainly to deviations in  $\rho_1$ , more marked in the HF range as shown in Fig. 2a, considering also that  $\epsilon_{r1}$  effects due to displacement current on cable propagation characteristics are evident at the HF region.

## IV. FD SOIL MODELING EFFECTS ON CABLE PROPAGATION CHARACTERISTICS

To demonstrate the impact of FD soil electrical properties on cable propagation characteristics the following ratio is employed for the LS formulation (7) and (8):

$$\text{ratio}(\omega) = \frac{|\text{propagation characteristics}_{FD}(\omega)|}{|\text{propagation characteristics}_{constant}(\omega)|}. \quad (14)$$

In the denominator of (14) Cases #1.1 and #2.1 are used as reference, since they represent the most commonly adopted soil models. The numerator also includes Cases #1.2 and #2.2.

### A. Earth formulation including earth admittance

In Figs. 4a, 4b and 4c the cable attenuation constant, velocity and characteristic impedance magnitude are

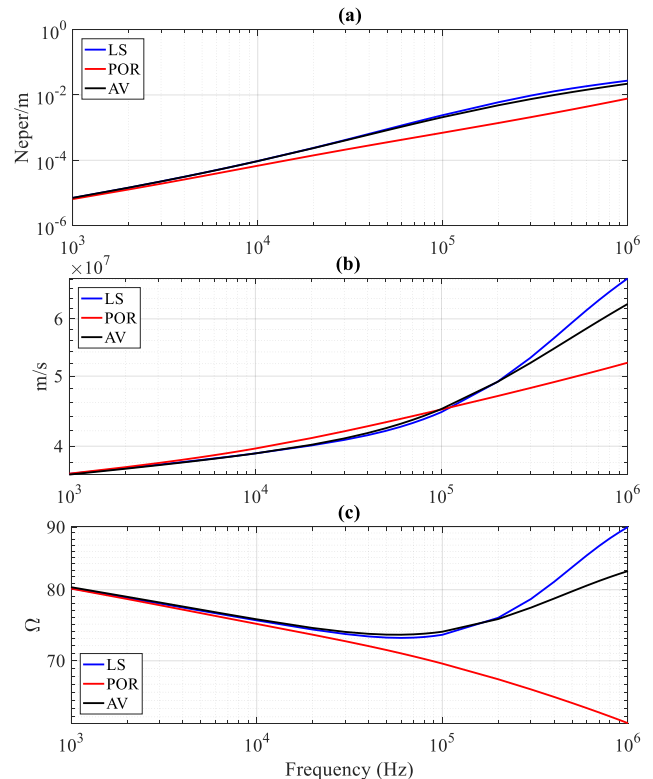


Fig. 3. SC cable (a) attenuation constant, (b) velocity and (c) characteristic impedance magnitude using different soil models; Case #2.3.

compared for Cases #1.1-#1.3; the corresponding ratios according to (14) are shown in Figs. 5a, 5b and 5c, respectively. The propagation characteristics are similar for frequencies up to some kHz. This frequency range is characterized by  $f_{cr-min}$ , estimated by [9]:

$$f_{cr-min} = 0.1\% \cdot f_{cr} = 0.1\% \cdot \sigma_1 / 2\pi\epsilon_0\epsilon_{r1} \quad (15)$$

Actually,  $f_{cr-min}$  can be used to describe the FD behavior of the earth in terms of resistive and displacement currents, since for lower frequencies the earth behaves as a conductor. As frequency increases the displacement and resistive currents become comparable and the earth behaves both as conductor and insulator, thus deviations in the propagation characteristics are observed especially for the attenuation constant, as shown in Figs. 4a and 5a. Finally, for frequencies higher than  $f_{cr}$  displacement currents start to dominate and the earth behaves mainly as an insulator [9].

Therefore, as the soil Cases shown in Figs. 4 and 5 are highly conductive ( $\rho_{1,LF} = 100 \Omega\text{m}$ ), the effects of  $\epsilon_{r1}$  on cable propagation characteristics are minimal. At HF the differences between the results of Cases #1.2 and #1.3 are mainly due to the frequency-dependent  $\rho_1$  for Case #1.3, since for Case #1.2  $\rho_1$  is constant.

In Fig. 6 the ratios of cable propagation characteristics are presented for Cases #2.2 and #2.3. Differences in propagation characteristics are more pronounced for these soil cases, since according to (15) displacement current is more important as earth resistivity increases. For frequencies above  $f_{cr-min}$  (~ some hundreds of Hz), the propagation characteristics between Cases #2.2 and #2.3 to #2.1 present significant differences.

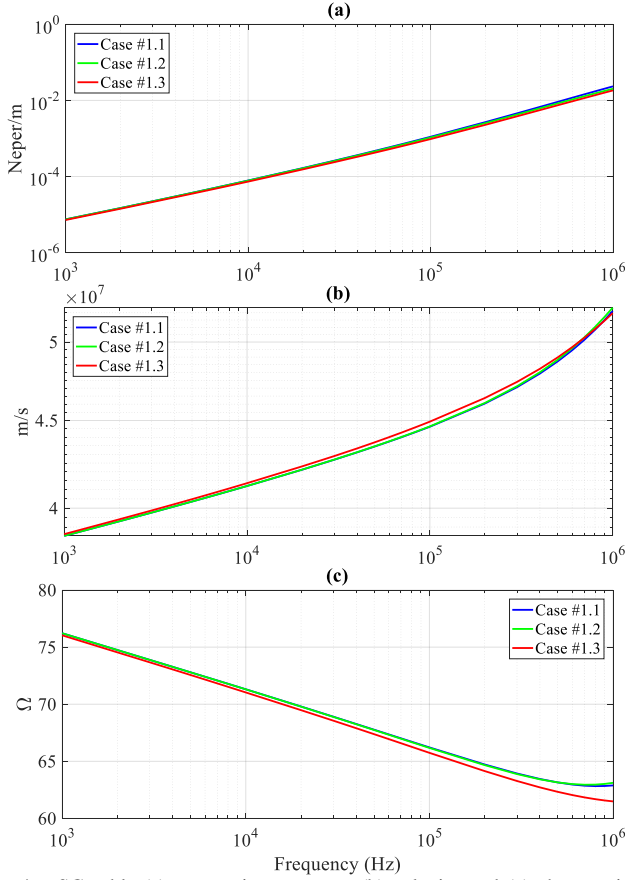


Fig. 4. SC cable (a) attenuation constant, (b) velocity and (c) characteristic impedance magnitude for Cases #1.1-#1.3.

In the HF region ( $f > f_{cr}$ ) the cable propagation characteristics are primarily affected by the displacement currents thus, accurate selection of the FD earth modeling approach is of major significance. In this region the propagation constant of the SC cable ( $\gamma_{HF}$ ) can be approximated with that of a bare wire ( $\gamma_{bare}$ ) [9]:

$$\gamma_{HF} = \sqrt{Z'_e \cdot Y'_e} \approx \gamma_{bare} = \sqrt{j\omega\mu_0(\sigma_1 + j\omega\epsilon_1)}. \quad (16)$$

Under this approximation:

- as  $\epsilon_{r1}$  increases the cable propagation attenuation constant as well as velocity decrease [8],
- considering a decreasing  $\rho_1$  with frequency, due to the FD behavior of soil, such as that shown in Fig. 2, the cable attenuation constant increases whereas velocity decreases with frequency.

These may explain the results of Figs. 3-5. In the HF region, as a result of the higher  $\epsilon_{r1}$ , the attenuation constant is lower for Cases #1.2, #1.3, #2.2 and #2.3 than Cases #1.1 and #2.1. Moreover, due to the significant reduction of  $\rho_1$  in the HF region, the attenuation constant is higher for Case #2.3 than Case #2.2 for frequencies higher than 400 kHz (Fig. 6).

### B. Approximate earth formulation

Fig. 7 shows the cable propagation characteristics for Cases #2.1-#2.3 calculated according to Sunde's [2] approximate approach, that is, by assuming wave propagation at LF. This is done using in (1)–(5) a propagation constant equal to zero ( $k'_x = 0$ ) and a perfectly conducting earth by neglecting the earth admittance term of (2) [3], [4].

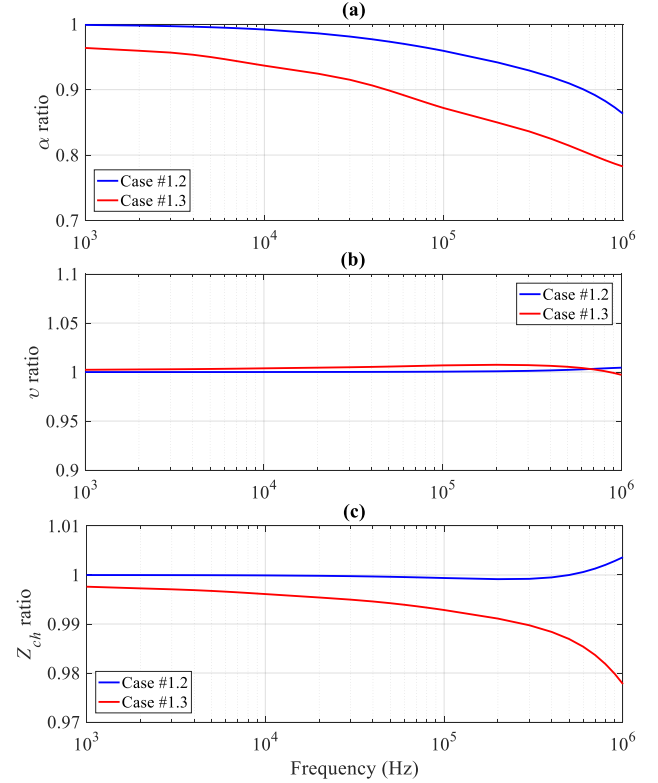


Fig. 5. Ratios of (a) attenuation constant, (b) velocity and (c) characteristic impedance magnitude for Cases #1.2 and #1.3.

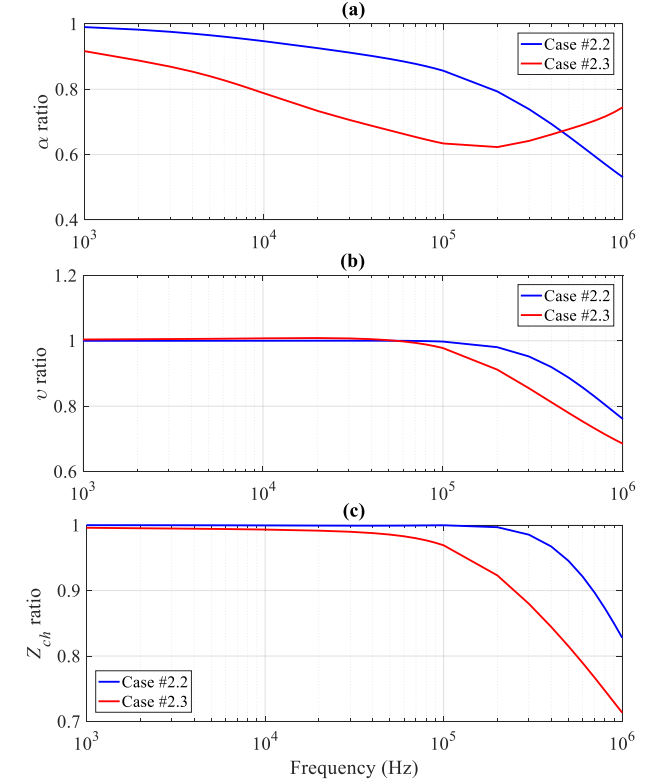


Fig. 6. Ratios of (a) attenuation constant, (b) velocity and (c) characteristic impedance magnitude for Cases #2.2 and #2.3.

As can be deduced from the comparison between Figs. 6 and 7 the calculated cable propagation characteristics show a significantly different behavior with frequency. The results obtained using Sunde's approach are not consistent with the EM field propagation in terms of (16); increasing  $\epsilon_{r1}$  results in increasing attenuation constant and velocity.

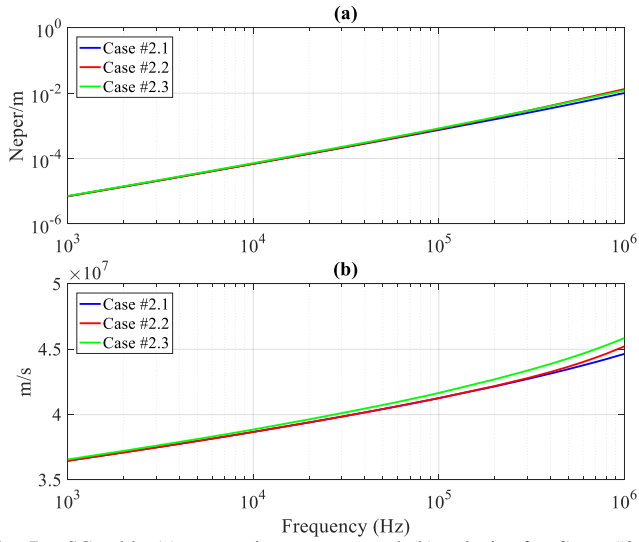


Fig. 7. SC cable (a) attenuation constant and (b) velocity for Cases #2.1-#2.3. Approximate earth formulation.

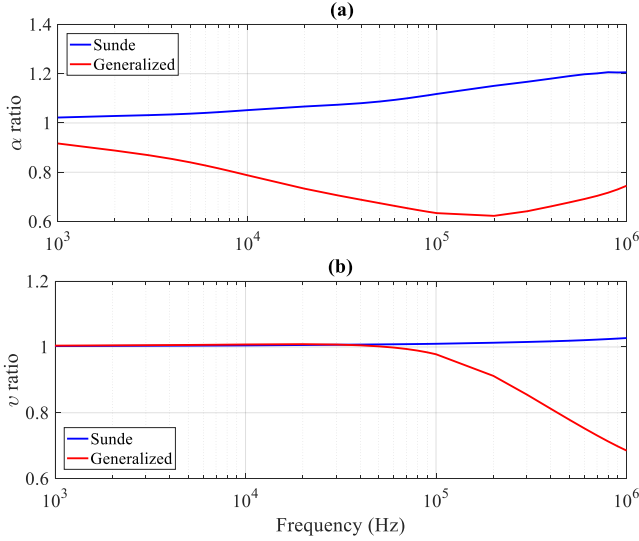


Fig. 8. Comparison of ratios for the (a) attenuation constant and (b) velocity between the proposed and approximate earth formulations. Case #2.3.

To further analyze the differences between the generalized and the approximate earth formulation the corresponding propagation characteristic ratios are compared in Fig. 8. It is evident that the propagation characteristics obtained by the generalized formulation are sensitive to soil FD dispersion; this is not the case for the results obtained by the approximate earth formulation.

## V. TRANSIENT RESPONSES

To demonstrate the effects of soil modeling on cable transient responses, a voltage source producing a standard lightning impulse (1.2/50  $\mu$ s waveform) of 1 pu amplitude is applied at the cable sending end  $S$ , with the receiving end  $R$ , open-ended. The transient responses are obtained for two cable lengths ( $\ell = 100$  and 1000 m) by using the transient simulation model introduced in [22] and the generalized earth formulation of (1) and (2) for calculating cable parameters. The natural frequency of the two cables was estimated about 110 kHz (100 m) and 10 kHz (1000 m) [23].

In Figs. 9a and 9b results are presented for soils Cases #1.1-#1.3. Small differences in transient responses are observed only for  $\ell = 100$  m. This is due to the fact that the natural frequency (110 kHz) of this cable is significantly higher than  $f_{cr-min}$ ; the latter is 4.2 kHz when the values at HF region of  $\rho_1 = 81 \Omega\text{m}$  and  $\epsilon_{r1} = 43$ , acquired using the LS soil model, are considered. This effect is more pronounced for soil Cases #2.1-#2.3, as can be seen in Fig. 10, because of a lower  $f_{cr-min}$  (1.38 kHz), the latter as obtained using the HF region values of  $\rho_1 = 568 \Omega\text{m}$  and  $\epsilon_{r1} = 23$ . For the same reason, differences up to  $\sim 10\%$  in transient responses are also observed for the cable with length 1000 m.

Finally, the transient responses at the cable end  $R$  obtained using the generalized and the Sunde's approximate earth formulations are presented in Fig. 11 for the soil Case #2.3. Noticeable differences are observed both in terms of voltage amplitude and attenuation rate for both cables, especially for the shortest one. Since the generalized earth formulation takes into account the earth admittance in cable parameters, the transient response so obtained shows a faster attenuation rate.

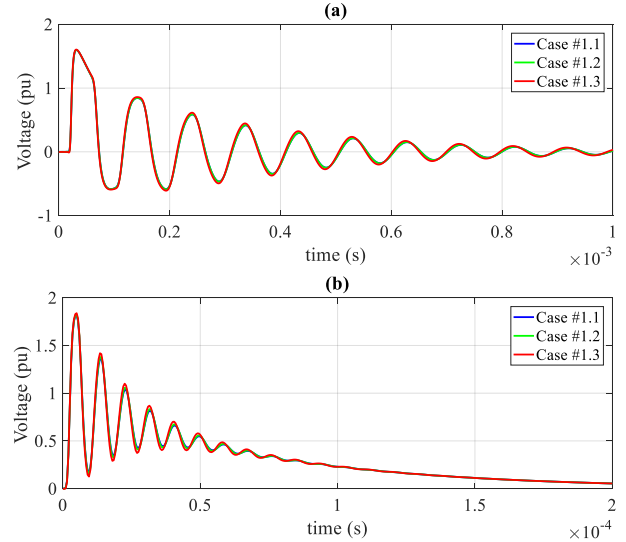


Fig. 9. Transient responses at end  $R$  for Cases #1.1-#1.3 and cable length equal to (a) 1000 m and (b) 100 m.

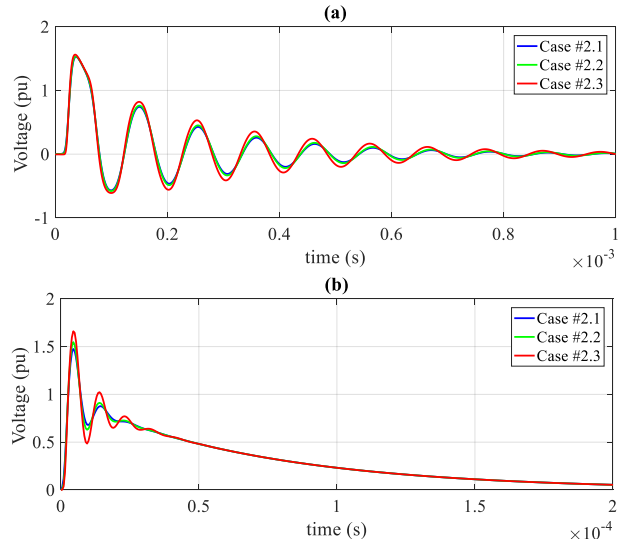


Fig. 10. Transient responses at end  $R$  for cases #2.1-#2.3 and cable length equal to (a) 1000 m and (b) 100 m.

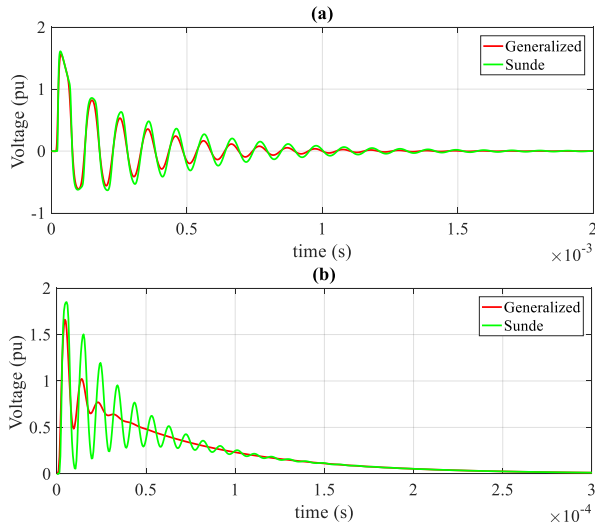


Fig. 11. Transient responses at end  $R$  for Case # 2.3 and cable length equal to (a) 1000 m and (b) 100 m.

## VI. CONCLUSIONS

The effects of the frequency-dependent (FD) soil electrical properties on the propagation characteristics and transient response of underground single core cables have been investigated, by considering several soils differing in electrical properties.

- Significant differences are observed in the predicted behavior of soil among the examined FD models. Generally, the divergence between the LF and HF  $\rho_1$  values is higher for soils of higher resistivity; such soils exhibit lower  $\varepsilon_{r1}$  values as well.
- The effects of using an FD soil model instead of one with constant soil properties on calculating cable propagation characteristics are significant. They are mainly attributed to the  $\rho_1$  dispersion, become more pronounced with  $\rho_{1,LF}$  and can be interpreted based on  $f_{cr-min}$ , below which displacement current has negligible influence.
- The influences of displacement current and FD soil properties on cable transient response depend on the cable length, becoming more evident for shorter lengths. As line length decreases the natural frequency of the line increases, thus more HF components are contained in the transient response.
- The cable propagation characteristics obtained using generalized formulations that consider the series impedance and shunt admittance are consistent with EM field propagation. Results obtained using approximate earth formulations show low sensitivity to the dispersion of soil electrical properties.

## VII. REFERENCES

- [1] F. Pollaczek, "Über das Feld einer unendlich langen wechselstromdurchflossenen Einfachleitung," *Elektr. Nachr. Technik*, vol. 3, no. 4, pp. 339-359, 1926.
- [2] E. D. Sunde, *Earth Conduction Effects in Transmission Systems*, 2nd ed., Dover Publications, 1968, pp. 99-139.
- [3] T. A. Papadopoulos, A. I. Chrysochos, and G. K. Papagiannis, "On the influence of earth conduction effects on the propagation characteristics of aerial and buried conductors," in *Proc. Int. Conf. Power Syst. Trans.*

- (*IPST2017*), Seoul, Republic of Korea, Jun. 2017.
- [4] N. Theethayi, R. Thottappillil, M. Paolone, C. A. Nucci, and F. Rachidi, "External impedance and admittance of buried horizontal wires for transient studies using transmission line analysis," *IEEE Trans. Dielectr. Electr. Insul.*, vol. 14, no. 3, pp. 751-761, Jun. 2007.
- [5] T. A. Papadopoulos, D. A. Tsiamitros, and G. K. Papagiannis, "Impedances and admittances of underground cables for the homogeneous earth case," *IEEE Trans. Power Del.*, vol. 25, no. 2, pp. 961-969, Apr. 2010.
- [6] A. P. C. Magalhães, M. T. C. de Barros, and A. C. S. Lima, "Earth return admittance effect on underground cable system modeling," *IEEE Trans. Power Del.*, vol. 33, no. 2, pp. 662-670, Apr. 2018.
- [7] H. Xue, A. Ametani, J. Mahseredjian, and I. Kocar, "Generalized formulation of earth-return impedance / admittance and surge analysis on underground cables," *IEEE Trans. Power Del.*, DOI: 10.1109/TPWRD.2018.2796089, early access, 2018.
- [8] T. A. Papadopoulos, D. A. Tsiamitros, and G. K. Papagiannis, "Analysis of the propagation characteristics of buried cables in imperfect earth," in *Proc. 2009 IEEE Bucharest PowerTech*, Bucharest, Romania, Jun.-Jul. 2009, pp. 1-8.
- [9] T. A. Papadopoulos, A. I. Chrysochos, and G. K. Papagiannis, "Analytical study of the frequency-dependent earth conduction effects on underground power cables," *IET Gener. Transm. Distrib.*, vol. 7, no. 3, pp. 276-287, Mar. 2013.
- [10] J. H. Scott, "Electrical and magnetic properties of rock and soil," Theoretical Notes, Note 18, Special Projects-16, Geological Survey, United States Department of the Interior, Federal Center, Denver, Colorado, USA, May 1966.
- [11] C. L. Longmire and K. S. Smith, "A universal impedance for soils," DNA 3788T, Mission Research Corporation, Santa Barbara, California, USA, Oct. 1975.
- [12] C. Portela, "Measurement and modeling of soil electromagnetic behavior," in *Proc. Int. Symp. Electromagn. Compat.*, Seattle, Washington, USA, Aug. 1999, vol. 2, pp. 1004-1009.
- [13] R. Alipio and S. Visacro, "Modeling the frequency dependence of electrical parameters of soil," *IEEE Trans. Electromagn. Compat.*, vol. 56, no. 5, pp. 1163-1171, Oct. 2014.
- [14] D. Cavka, N. Mora, and F. Rachidi, "A comparison of frequency-dependent soil models: Application to the analysis of grounding systems," *IEEE Trans. Electromagn. Compat.*, vol. 56, no. 1, pp. 177-187, Feb. 2014.
- [15] A. C. S. de Lima and C. Portela, "Inclusion of frequency-dependent soil parameters in transmission-line modeling," *IEEE Trans. Power Del.*, vol. 22, no. 1, pp. 492-499, Jan. 2007.
- [16] M. M. Y. Tomasevich and A. C. S. Lima, "Impact of frequency-dependent soil parameters in the numerical stability of image approximation-based line models," *IEEE Trans. Electromagn. Compat.*, vol. 58, no. 1, pp. 323-326, Feb. 2016.
- [17] M. A. O. Schroeder, M. T. C. de Barros, A. C. S. Lima, M. M. Afonso, and R. A. R. Moura, "Evaluation of the impact of different frequency dependent soil models on lightning overvoltages," *Electr. Power Syst. Res.*, vol. 159, pp. 40-49, Jun. 2018.
- [18] J. Paknahad, K. Sheshyekani, F. Rachidi, M. Paolone, and A. Mimouni, "Evaluation of lightning-induced currents on cables buried in a lossy dispersive ground," *IEEE Trans. Electromagn. Compat.*, vol. 56, no. 6, pp. 1522-1529, Dec. 2014.
- [19] E. F. Vance, *Coupling to Shielded Cables*, John Wiley and Sons, 1978.
- [20] Z. G. Datsios and P. N. Mikropoulos, "Characterization of the frequency dependence of the electrical properties of sandy soil with variable grain size and water content," *IEEE Trans. Dielectr. Electr. Insul.* (accepted for publication).
- [21] Z. G. Datsios, P. N. Mikropoulos, and I. Karakousis, "Laboratory measurement of the low-frequency electrical properties of sand," in *Proc. 34th Int. Conf. Lightn. Prot. (ICLP)*, Rzeszow, Poland, Sep. 2018.
- [22] A. I. Chrysochos, T. A. Papadopoulos, and G. K. Papagiannis, "Enhancing the frequency-domain calculation of transients in multiconductor power transmission lines," *Electr. Power Syst. Res.*, vol. 122, pp. 56-64, May 2015.
- [23] A. I. Chrysochos, T. A. Papadopoulos, and G. K. Papagiannis, "A rigorous calculation method for resonance frequencies in transmission line responses," *IET Gener. Transm. Distrib.*, vol. 9, no. 8, pp. 767-778, May 2015.